Published September 10, 2007

Defective microtubule-dependent podosome organization in osteoclasts leads to increased bone density in *Pyk2*$^{-/-}$ mice

Hava Gil-Henn,[1] Olivier Destaing,[2] Natalie A. Sims,[2] Kazuhiro Aoki,[2,3] Neil Alles,[3] Lynn Neff,[2] Archana Sanjay,[2] Angela Bruzzaniti,[2] Pietro De Camilli,[2] Roland Baron,[2] and Joseph Schlessinger[1]

[1]Department of Pharmacology, Yale University School of Medicine, New Haven, CT 06511
[2]Departments of Cell Biology and Orthopaedics, Yale University School of Medicine, New Haven, CT 06511
[3]Department of Hard Tissue Engineering, Section of Pharmacology, Graduate School, Tokyo Medical and Dental University, Tokyo 113-8549, Japan

The protein tyrosine kinase Pyk2 is highly expressed in osteoclasts, where it is primarily localized in podosomes. Deletion of *Pyk2* in mice leads to mild osteopetrosis due to impairment in osteoclast function. *Pyk2*-null osteoclasts were unable to transform podosome clusters into a podosome belt at the cell periphery; instead of a sealing zone only small actin rings were formed, resulting in impaired bone resorption. Furthermore, in *Pyk2*-null osteoclasts, Rho activity was enhanced while microtubule acetylation and stability were significantly reduced. Rescue experiments by ectopic expression of wild-type or a variety of Pyk2 mutants in osteoclasts from *Pyk2*$^{-/-}$ mice have shown that the FAT domain of Pyk2 is essential for podosome belt and sealing zone formation as well as for bone resorption. These experiments underscore an important role of Pyk2 in microtubule-dependent podosome organization, bone resorption, and other osteoclast functions.

Introduction

The protein tyrosine kinase Pyk2 (also designated RAFTK, CADTK, and CTK) and FAK are two members of a distinct family of nonreceptor tyrosine kinases. PYK2 and FAK share ~45% amino acid sequence identity and a common domain structure: an N-terminal FERM domain followed by a protein tyrosine kinase (PTK) domain, three proline-rich regions, and a focal adhesion targeting (FAT) domain at the C terminus. Although FAK is expressed in most cells (Richardson and Parsons, 1996), Pyk2 exhibits a more restricted expression pattern with strongest expression in the central nervous system and in hematopoietic cells (Lev et al., 1995). FAK is a major intracellular signaling component of integrin-mediated cell adhesion (Schlaepfer et al., 1999) and plays a role in signaling pathways mediated by growth factor receptors. PYK2, on the other hand, is activated by a variety of extracellular cues including agonists of G protein–coupled receptors, intracellular Ca^{+2} concentration, inflammatory cytokines, and stress signals, as well as integrin-mediated cell adhesion (Lev et al., 1995; Schlaepfer et al., 1999).

Pyk2 is highly expressed in osteoclasts, where it is primarily confined to podosomes (Duong et al., 1998; Williams and Ridley, 2000; Pfaff and Jurdic, 2001). Podosomes are highly dynamic, actin-rich structures that mediate cell attachment and migration of highly motile cells such as macrophages and osteoclasts. They are composed of a central actin-bundle core surrounded by integrins and integrin-associated adhesion molecules (Linder and Aepfelbacher, 2003). When plated on glass, mature osteoclasts organize their podosomes at the periphery of the cell in a large belt-like structure. The podosome belt is similar to the sealing zone, another podosome-containing structure that is formed in active bone-resorbing osteoclasts (Luxenburg et al., 2007). Both structures share the same molecular components and are stabilized by microtubules (Destaing et al., 2003, 2005). Reduction of Pyk2 expression in osteoclasts by adenovirus containing Pyk2 antisense RNA leads to impairment in integrin-mediated cytoskeletal organization and bone resorption (Duong et al., 2001). In addition, macrophages from *Pyk2*$^{-/-}$ mice failed

H. Gil-Henn and O. Destaing contributed equally to this paper.

Correspondence to Joseph Schlessinger: joseph.schlessinger@yale.edu; or Roland Baron: roland.baron@yale.edu.

N.A. Sims' present address is St. Vincent's Institute, Fitzroy VIC 3065, Victoria, Australia.

K. Aoki's present address is Department of Hard Tissue Engineering, Section of Pharmacology, Graduate School, Tokyo Medical and Dental University, Tokyo 113-8549, Japan.

A. Sanjay's present address is Department of Anatomy and Cell Biology, Temple University School of Medicine, Philadelphia, PA 19140.

Abbreviations used in this paper: FAT, focal adhesion targeting; RBD, Rho binding domain.

The online version of this article contains supplemental material.

Supplemental Material can be found at:
http://jcb.rupress.org/content/suppl/2007/09/10/jcb.200701148.DC1.html

The Journal of Cell Biology, Vol. 178, No. 6, September 10, 2007 1053–1064
http://www.jcb.org/cgi/doi/10.1083/jcb.200701148

Published September 10, 2007

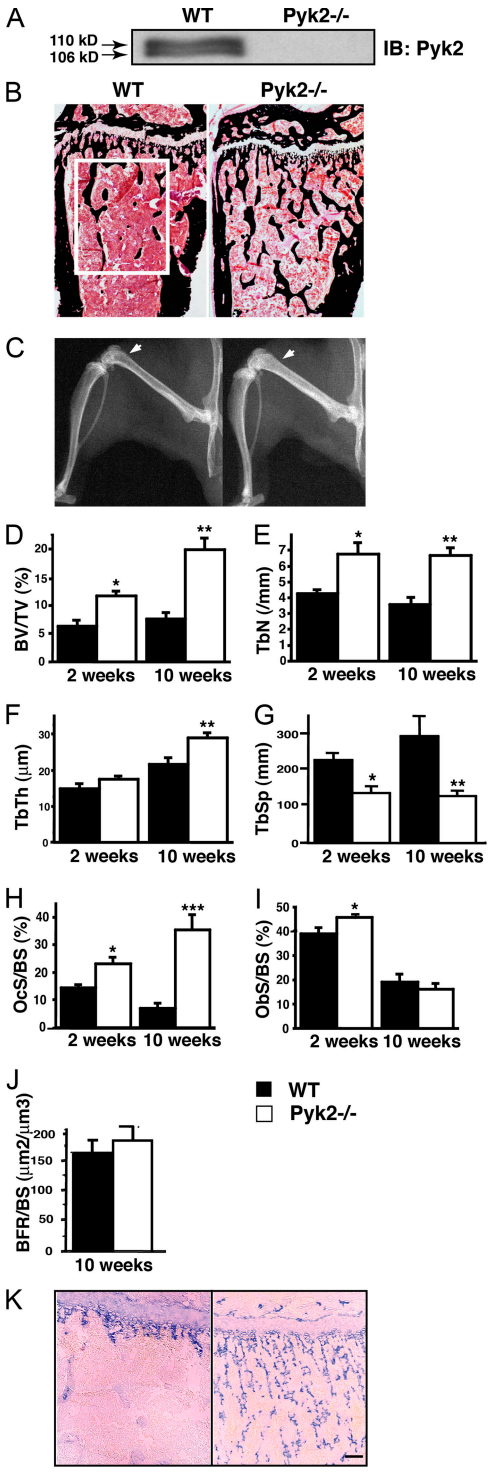

Figure 1. ***Pyk2*$^{-/-}$ mice are osteopetrotic.** (A) Immunoblotting of protein lysates from wild-type and *Pyk2*-null osteoclasts using anti-Pyk2 antibodies. Top band is the ubiquitous isform of Pyk2 and the bottom band is the Pyk2 isoform expressed in hematopoietic cells. (B) Longitudinal section of representative tibiae from 10-wk-old wild-type and *Pyk2*$^{-/-}$ mice, stained according to the method of Von Kossa. The color of mineralized matrix is black. White square shows the metaphyseal region used for histomorphometry. (C) X-ray analysis of tibiae and femora from 10-wk-old wild-type and *Pyk2*$^{-/-}$ mice. Notice increased bone density in the femoral metaphysis of *Pyk2*$^{-/-}$ mice, compared with wild-type (arrowhead). (D–J) Quantitative histomorphometry of proximal tibiae from 2- and 10-wk-old wild-type (black) and *Pyk2*$^{-/-}$ (white) mice. BV/TV, trabecular bone volume (% bone volume) (d); TbN, trabecular number (e); TbTh, trabecular thickness (f); TbSp, trabecular spacing (g); OcS/BS, osteoclast surface (% of bone surface) (h); ObS/BS, osteoblast surface (% of bone surface) (i); BFR/BS, bone formation rate (j). Bars show means ± SEM. n = 8–10 for each group, *, $P < 0.05$; **, $P < 0.01$; ***, $P < 0.001$, as determined by two-way ANOVA. (K) Alcian blue staining of proximal tibial growth plates from 10-wk-old wild-type and *pyk2*$^{-/-}$ mice. Note the un-remodeled cartilage in the trabecular bone of *Pyk2*$^{-/-}$ mice (blue). Bar, 20 μm.

to become polarized and to migrate in response to chemokine stimulation in vitro and in vivo (Okigaki et al., 2003). It has been proposed that a ternary Pyk2-Src-Cbl complex induced by integrin engagement plays an important role in the control of osteoclast migration and bone resorption (Sanjay et al., 2001; Miyazaki et al., 2004). However, it is not clear how signaling via Pyk2 is linked to changes in the osteoclast cytoskeleton, and in particular to podosome assembly and organization, processes required for bone resorption.

Here, we report that Pyk2 deficiency in mice leads to an osteopetrotic phenotype. Osteoclasts from *Pyk2*$^{-/-}$ mice are defective in cell polarization, fail to form proper sealing zones, and inefficiently resorb dentin in vitro. Furthermore, *Pyk2*-null osteoclasts fail to form a podosome belt that is typically seen at the periphery of wild-type osteoclasts. We also demonstrate that Rho activity is increased and the cellular distribution and stability of microtubules are compromised in *Pyk2*-null osteoclasts. Ectopic expression of wild-type or Pyk2 mutants in *Pyk2*-null osteoclasts demonstrates that the FAT domain of Pyk2 plays a primary role in the control of podosome belt and sealing zone formation, as well as in bone resorption. These experiments show that Pyk2, by controlling Rho activity, regulates microtubule-dependent podosome organization in osteoclasts and thereby bone resorption.

Results

Pyk2$^{-/-}$ mice are osteopetrotic

We have previously described the generation of *Pyk2*$^{-/-}$ mice and demonstrated that Pyk2 deficiency results in impairment in multiple macrophage functions (Okigaki et al., 2003). Because Pyk2 is abundantly expressed in osteoclasts, we have examined the possibility of whether deficiency in Pyk2 may result in bone abnormalities. Immunoblotting of osteoclast lysates with anti-Pyk2 antibodies revealed the presence of both the ubiquitous (110 kD) and hematopoietic (106 kD) Pyk2 isoforms, which have been shown to be generated by alternative RNA splicing (Dikic et al., 1998) (Fig. 1 A). Histological and histomorphometric comparison showed that the size and shape of bones from *Pyk2*$^{-/-}$ mice are normal. The length and width of the femur at the metaphyseal mid-point of either 2- or 10-wk-old mice were similar, and no changes were detected in the proliferative or hypertrophic zones of growth plates (unpublished data). However, the density of bones of either 2- or 10-wk-old *Pyk2*$^{-/-}$ mice was substantially elevated throughout the skeleton as shown by X-ray analysis and by histology (Fig. 1, B and C). Histomorphometric analysis demonstrated higher trabecular bone volume in *Pyk2*$^{-/-}$ mice (Fig. 1 D). The increase in trabecular bone volume is largely due to increased trabecular number (Fig. 1 E) and to a

Published September 10, 2007

lesser extent to increased trabecular thickness, more evident in 10-wk-old *Pyk2*$^{-/-}$ mice (Fig. 1 F), whereas trabecular spacing was reduced at both time points (Fig. 1 G).

Although trabecular bone volume was high, the percentage of trabecular bone surface covered by osteoclasts (osteoclast surface) was substantially elevated in *Pyk2*$^{-/-}$ mice, by 60% in 2-wk-old mice, and by nearly 300% in 10-wk-old mice (Fig. 1 H). Elevated osteoclast surface in the presence of high trabecular bone volume suggests a defect in osteoclast function, as shown in several osteopetrotic mutants (Soriano et al., 1991; McHugh et al., 2000; Hollberg et al., 2002). Gain of trabecular bone volume may also result from high bone formation caused by changes in osteoblast differentiation or function. A mildly elevated osteoblast surface (percentage of trabecular bone covered by osteoblasts) was detected in 2-wk-old *Pyk2*$^{-/-}$ mice, but both osteoblast surface and bone formation rates (determined by measuring incorporation of calcium-binding fluorochromes) were normal in 10-wk-old mice (Fig. 1, I and J, respectively), while their trabecular bone volume continued to increase. Although at this time we cannot completely rule out a minor effect of Pyk2 deficiency on osteoblast function, our results strongly support the notion that impairment in osteoclast function is the primary cause of the bone phenotype of *Pyk2*$^{-/-}$ mice. Indeed, and strongly supporting this conclusion, abundant cartilage remnants were detected in the trabeculae of 10-wk-old *Pyk2*$^{-/-}$ mice (Fig. 1 K). This may result from defective resorption of the growth plate cartilage, and is an important hallmark of osteopetrosis (Walker, 1975; Helfrich et al., 1991).

Pyk2-null osteoclasts exhibit a cell-autonomous defect in bone resorption

To examine whether the osteopetrosis of *Pyk2*$^{-/-}$ mice is indeed caused by defective osteoclast function, osteoclasts isolated from wild-type or *Pyk2*$^{-/-}$ mice were plated on dentin, and their ability to form pits was compared. After 48 h, the area, depth, and volume of the pits were compared using three-dimensional scanning confocal microscopy. The volume of dentin excavated by *Pyk2*-null osteoclasts was significantly reduced (Fig. 2 A). The decrease in pit volume resulted from a decrease in both area and depth; the pits formed by *Pyk2*-null osteoclasts were more shallow (Fig. 2, A and B). Thus, in the absence of Pyk2, osteoclasts show a cell-autonomous decrease in bone-resorbing activity.

To gain further insight into the mechanism underlying the reduced resorption by *Pyk2*-null osteoclasts, we compared the distribution and status of cytoskeletal proteins in osteoclasts from wild-type or *Pyk2*$^{-/-}$ mice. Immunofluorescence microscopy of osteoclasts plated on dentin and stained with fluorescently labeled phalloidin demonstrated that *Pyk2*-null

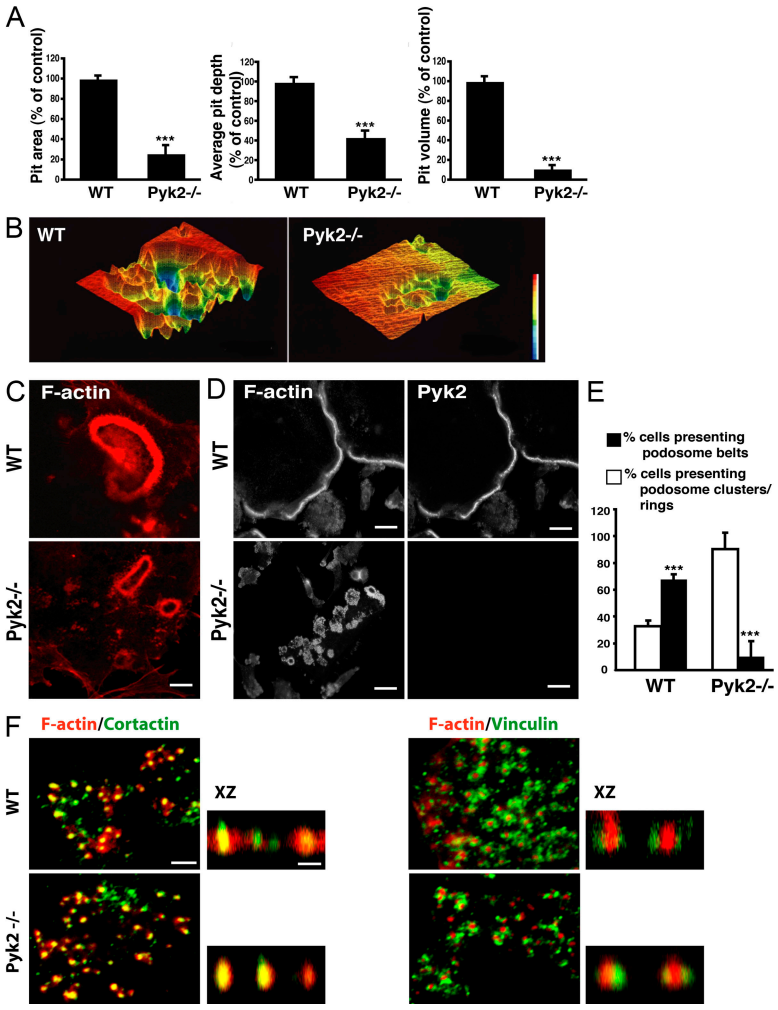

Figure 2. **Defective bone resorption and altered cytoskeletal organization in *Pyk2*-null osteoclasts.** (A) Osteoclasts isolated from wild-type and *Pyk2*-null mice were plated on dentin slices and allowed to excavate pits. Average area, depth, and volume of pits resorbed by wild-type and *Pyk2*-null osteoclasts were measured and analyzed using a violet laser color 3D profile confocal microscope. Data are presented as means ± SD; $n = 6$ from two individual experiments, ***, $P < 0.001$ as determined by *t* test. (B) Views of resorption pits from randomly chosen sites in dentin slices resorbed by wild-type or *Pyk2*-null osteoclasts, as viewed by color laser 3D profile confocal microscope. Blue color represents deeper resorbed area, red represents a more shallow region. (C) Disrupted polarization of *Pyk2*-null osteoclasts on bone. Authentic osteoclasts were isolated from wild-type and *Pyk2*-null newborn mice, plated on dentin slices, and allowed to resorb. Cells on slices were fixed and labeled for F-actin (shown in red). Bar, 10 μm. (D) *Pyk2*-null osteoclasts show podosome clusters and rings but almost no belts. Wild-type and *Pyk2*-null spleen-derived osteoclasts were differentiated on coverslips for 8 d, fixed, and labeled for F-actin (left) and Pyk2 (right). Note clusters and small rings in *Pyk2*-null osteoclasts (bottom left), as opposed to peripheral podosome belt in wild-type cells, in which Pyk2 is localized (two top panels). Bar, 20 μm. (E) Quantification of percentage of cells with podosome clusters/rings (white) and belts (black) in wild-type and *Pyk2*-null osteoclasts from two individual experiments performed as above. A total of 1,500 osteoclasts were counted. Results are presented as means ± SD, ***, $P < 0.001$ as determined by *t* test. (f) Co-localization of cortactin or vinculin with actin in podosome clusters from wild-type and *Pyk2*-null osteoclasts (left panels) and XZ series (longitudinal view) of individual podosomes (right panels). Bar, 15 μm in left panel and 1 μm in XZ panel.

Published September 10, 2007

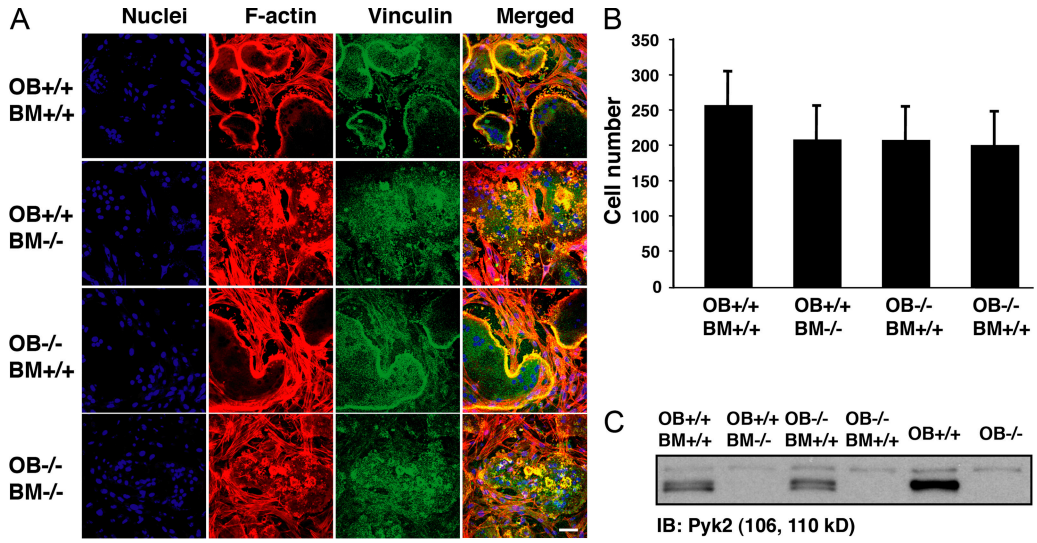

Figure 3. ***Pyk2*-null osteoclasts are inherently defective.** Osteoblasts from wild-type or *Pyk2*$^{-/-}$ mice were co-cultured with bone marrow cells of either genotype, and allowed to differentiate in culture. (A) Fluorescence micrographs of the cells showing multiple nuclei of differentiated osteoclasts (blue), F-actin (red), and vinculin (green). Bar, 20 μm. (B) Parallel cocultures were stained for TRAP, and TRAP-positive cells containing three or more nuclei were counted. Experiment was preformed in triplicate and repeated twice with similar results. (C) Pyk2 expression in cells. Osteoblasts were separated from osteoclasts by gentle pipetting and lysates from the osteoblasts and osteoclasts were subjected to immunoblotting with anti-Pyk2 antibodies.

osteoclasts formed an abnormal, thinner and smaller sealing zone (Fig. 2 C). Furthermore, immunofluorescent labeling of osteoclasts plated on glass demonstrated that in wild-type osteoclasts, F-actin was primarily localized in a podosome belt at the periphery of the cells, whereas in osteoclasts from *Pyk2*$^{-/-}$ mice, actin was organized in podosome clusters and multiple small rings throughout the cell (Fig. 2, D and E). Cellular localization of actin, cortactin, vinculin, and paxillin in podosomes using fluorescence microscopy have demonstrated that their distribution is similar in wild-type and *Pyk2*-null podosomes (Fig. 2 F and Fig. S1, available at http://www.jcb.org/cgi/content/full/jcb.200701148/DC1). These experiments show that in absence of Pyk2, podosomes fail to organize in a belt-like structure at the periphery of the cell. The defect in organization of podosomes also correlates with the presence of abnormal sealing zones in *Pyk2*-null osteoclasts, which may explain the shallower resorption cavities formed by *Pyk2*-null osteoclasts in vitro.

The defect of *Pyk2*-null osteoclasts is not osteoblast dependent

To further determine whether the defect in *Pyk2*-null osteoclasts is cell autonomous, we co-cultured different combinations of wild-type or *Pyk2*-null bone marrow cells and calvarial osteoblasts, allowing marrow-derived osteoclast precursor cells to differentiate into osteoclasts (Takahashi et al., 1988). As shown in Fig. 3, absence of podosome belt, revealed by both F-actin and vinculin staining, was detected in osteoclasts derived from *Pyk2*$^{-/-}$ marrow whether in the presence of wild-type or *Pyk2*-null osteoblasts (Fig. 3 A). The number of osteoclasts generated from *Pyk2*$^{-/-}$ bone marrow was not significantly different from wild-type, regardless of the origin of the supporting osteoblasts (Fig. 3 B). Collectively, these results demonstrate that osteoclast differentiation is unaffected by the absence of Pyk2, and that the functional defect in *Pyk2*-null osteoclasts is cell autonomous.

Actin and podosome dynamics are altered in *Pyk2*-null osteoclasts

The dynamic nature of GFP-labeled actin that was expressed in osteoclasts from wild-type or *Pyk2*$^{-/-}$ mice was compared by fluorescence recovery after photobleaching (FRAP) measurements (Axelrod et al., 1976). Characteristic photobleaching recovery time of GFP-actin in wild-type osteoclasts was ∼30 s, as described previously (Destaing et al., 2003). In contrast, the photobleaching recovery time of GFP-actin in *Pyk2*-null osteoclasts was doubled (Fig. 4 A), indicating that the rate of actin flux in podosomes is reduced in the absence of Pyk2. The molecular mechanisms underlying the observed differences in FRAP measurements is currently unknown. Notwithstanding the decreased rate of actin flux in individual podosomes, the total podosome life-span (namely, the average time from the first appearance of a new podosome to its dissociation) in osteoclasts expressing GFP-actin was not significantly different (Fig. 4 B). Overall, these results suggest that in osteoclasts, Pyk2 contributes to the dynamic exchange of actin in podosomes, but not to podosome life span. The podosome organization defects in *Pyk2*-null osteoclasts, which prevent podosome belt formation, are unlikely to be caused by a change in podosome life span in these cells.

Microtubule stability and acetylation are altered in osteoclasts from *Pyk2*$^{-/-}$ mice

Previous analyses have shown that the process of podosome patterning is controlled by the microtubule network in osteoclasts (Destaing et al., 2003). During podosome differentiation, podosomes initially organize into clusters that evolve into unstable small podosome rings by a mechanism of self-organization. Subsequently, the small rings fuse and expand by an oriented treadmilling process toward the periphery of the cell to form belts. Thus, the pattern of podosomes in *Pyk2*-null osteoclasts

Published September 10, 2007

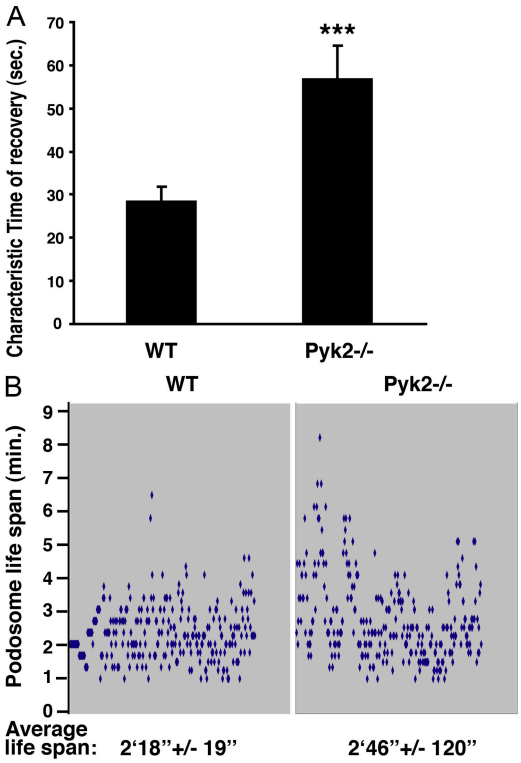

Figure 4. **Actin and podosome dynamics in wild-type and *Pyk2*-null osteoclasts.** (A) FRAP analysis of podosomes of wild-type or *Pyk2*-null osteoclasts. Mature osteoclasts were microinjected with expression vector for GFP-actin, after which GFP-actin in podosome clusters was photobleached in defined regions (a rectangle of 5 × 2.5 μm) and allowed to recover. The time of recovery of fluorescence in single podosomes that existed during the whole recovery time was measured, and the average characteristic time of recovery was calculated for podosomes in wild-type and *Pyk2*-null cells. (characteristic time of recovery refers to the inverse of the constant k_2 ($1/k_2$ in the equation $I(t) = I_{(0)} + k_1 e^{k}{}_2{}^{t}$, used to fit the curve of fluorescence recovery). 45 measurements per condition in 13 cells each were analyzed, in two independent experiments. Results are presented as means ± SD. ***, $P < 0.01$ as determined by *t* test. (B) Differentiated wild-type and *Pyk2*-null osteoclasts were microinjected with expression vector for GFP-actin and observed by time-lapse microscopy. Individual podosomes in clusters were followed, and their life span (the overall time in which a fluorescently labeled podosome exists), was calculated and plotted. 150 measurements of each wild-type and *Pyk2*-null osteoclasts were performed, from a total of 6–7 cells each, in two independent experiments. Results are presented as means ± SD.

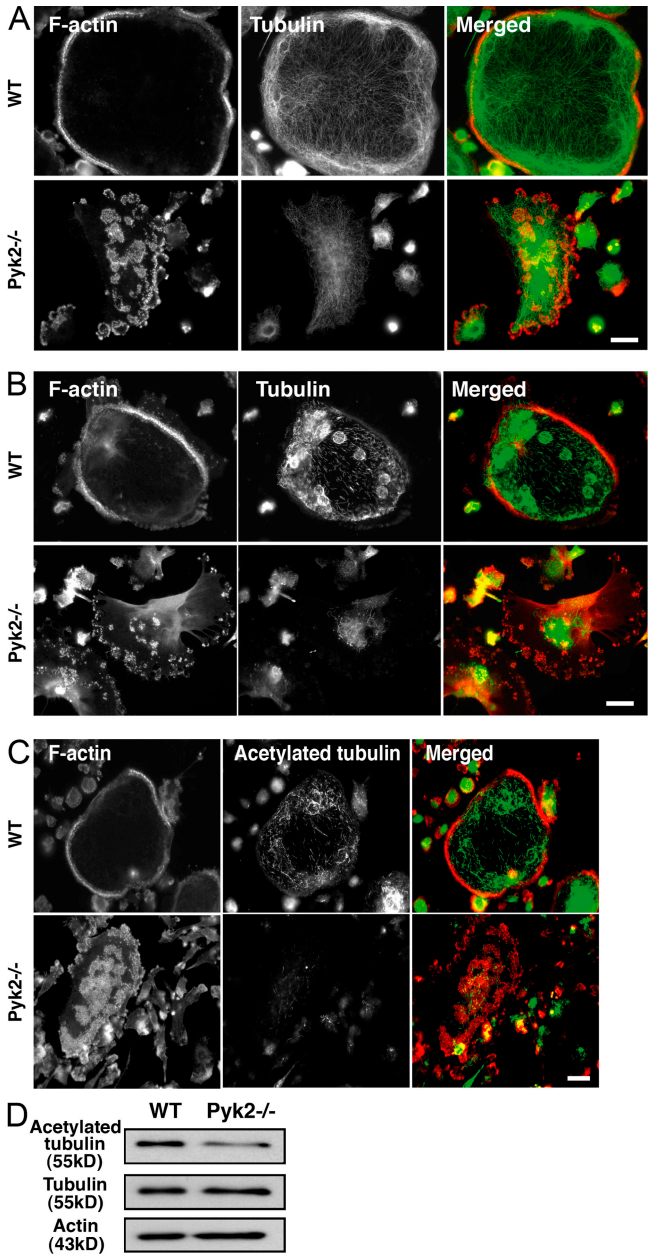

Figure 5. **Microtubule stability and acetylation are altered in *Pyk2*-null osteoclasts.** (A) Wild-type or *Pyk2*-null osteoclasts were fixed, permeabilized, and labeled with rhodamine-phalloidin (red) or anti-tubulin antibodies (green). Bar, 15 μm. (B) Differentiated wild-type and *Pyk2*-null osteoclasts were treated for 45 min in 2 μM nocodazole, fixed, and labeled with rhodamine-phalloidin (left panels) or anti-tubulin antibodies (center panels). Bar, 15 μm. (C) Mature wild-type and *Pyk2*-null osteoclasts were fixed, permeabilized, and labeled with rhodamine-phalloidin (red) or with anti-acetylated tubulin antibodies (green). Bar, 15 μm. (D) Cell lysates from wild-type or *Pyk2*-null osteoclasts were immunoblotted with anti-acetylated tubulin antibodies (top). The blot was stripped and re-probed with anti-tubulin (middle) and anti-actin (bottom) antibodies, for loading controls.

resembles earlier stages of osteoclast differentiation, when podosomes are organized in clusters and small, dynamic podosome rings. It was demonstrated that the transition of clusters/rings to peripheral podosome belt requires an intact microtubule network (Destaing et al., 2003). We therefore analyzed microtubule distribution and found that *Pyk2*-null osteoclasts lacked the characteristic circular microtubule network that is concentrated around the podosome belt in normal cells (Turksen et al., 1988; Destaing et al., 2003), while maintaining the radial network of microtubules (Fig. 5 A).

Cellular microtubules are composed of two distinct pools with regard to their stability: a short-lived pool with a half-life of ~5–10 min and a more stable pool that may last for as long as several hours. The stable microtubule pool is resistant to treatment with the microtubule-depolymerizing agent nocodazole and contributes to podosome belt stabilization in osteoclasts (Westermann and Weber, 2003; Destaing et al., 2005). As expected, wild-type osteoclasts contained a nocodazole-resistant pool of stable microtubules. In contrast, very few nocodazole-resistant microtubules were seen in *Pyk2*-null osteoclasts, demonstrating that the short-lived, rather than the stable pool, is the predominant form of microtubules in cells lacking Pyk2 (Fig. 5 B).

Published September 10, 2007

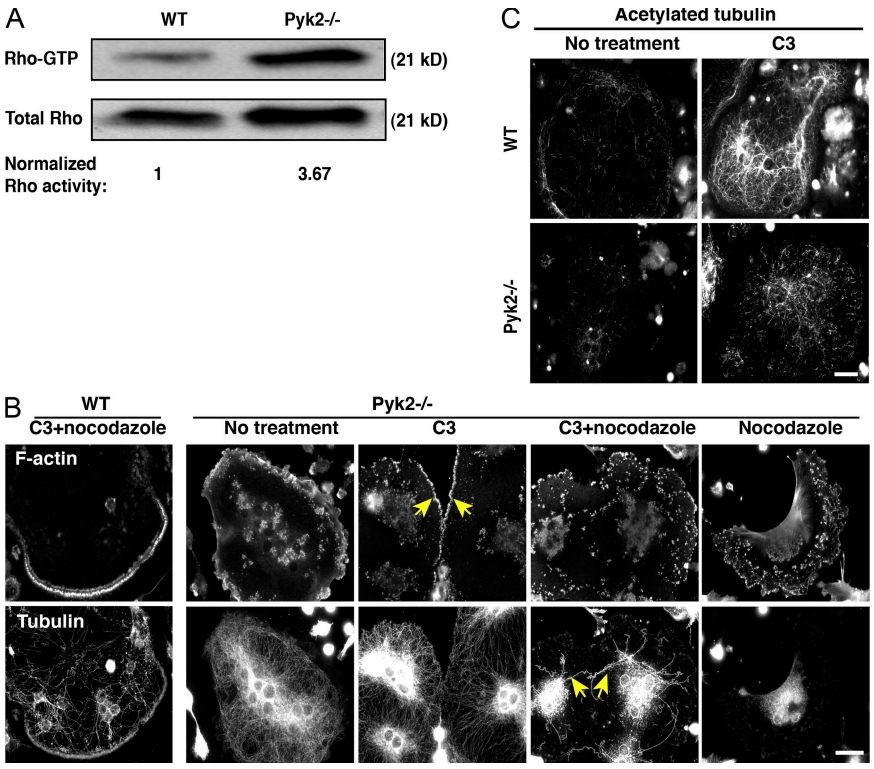

Figure 6. **Enhanced Rho activity and reduced microtubule acetylation in *Pyk2*-null osteoclasts.** (A) Lysates from wild-type or *Pyk2*-null osteoclasts were subjected to a pull-down assay using GST-RBD. The amount of RBD-bound Rho and total Rho in cell lysates was determined by immunoblotting with anti-Rho antibodies. The ratio of GTP-bound Rho to total Rho was determined by densitometry. Shown is a representative of three individual experiments. (B) Rho inhibition by C3 toxin promotes podosome belt formation and microtubules stabilization in *Pyk2*-null osteoclasts. *Pyk2*-null osteoclasts were left untreated, or treated with 5 μg/ml C3 for 5.5 h with or without 2 μM nocodazole for the last 35 min. Cells were fixed and labeled with rhodamine-phalloidin (top) or anti-tubulin antibodies (bottom). Wild-type cells were treated with C3 and nocodazole, as control (left). Note the appearance of podosomes in a belt-like structure in *Pyk2*-null osteoclasts after C3 treatment (arrows, middle panel, top) and appearance of nocodazole-resistant microtubules in *Pyk2*-null osteoclasts treated with C3 plus nocodazole (compare two bottom panels in bottom right). Bar, 15 μm. (C) Wild-type and *Pyk2*-null osteoclasts were treated with C3 as described above, fixed, permeabilized, and labeled with anti-acetylated tubulin antibodies. Bar, 15 μm.

Because the stable pool of microtubules that accumulates during osteoclastogenesis is highly acetylated (Destaing et al., 2005), we next analyzed microtubule acetylation by immunofluorescence microscopy of permeabilized cells labeled with antibodies specific for the acetylated form of tubulin. This experiment showed that microtubule acetylation is reduced in *Pyk2*-null osteoclasts (Fig. 5 C). A similar conclusion was drawn by immunoblotting experiments demonstrating that acetylation of microtubules is, indeed, compromised in *Pyk2*$^{-/-}$ osteoclasts (Fig. 5 D). The reduced acetylation of microtubules in *Pyk2*-null osteoclasts is consistent with their reduced stability, as revealed by nocodazole treatment. It was shown that microtubule acetylation is regulated by the mDia2-HDAC6 complex in osteoclasts (Destaing et al., 2005). However, analyses of mDia2 localization in wild-type and *Pyk2*-null osteoclasts using fluorescence microscopy revealed similar cellular distribution (Fig. S4, available at http://www.jcb.org/cgi/content/full/jcb.200701148/DC1).

Enhanced Rho activity in *Pyk2*-null osteoclasts

The small GTPase Rho has been implicated in the stabilization and post-translational modification of microtubules (Palazzo et al., 2004). In addition, Rho inhibition leads to enhancement in the acetylation and stabilization of the microtubule network in osteoclasts (Destaing et al., 2005). To examine the possibility of whether the reduced stability and acetylation of microtubules in *Pyk2*-null osteoclasts are caused by increased Rho activation, Rho activity was determined by using a GST fusion protein containing the Rho binding domain of Rhotekin (RBD) to pull down the active, GTP-bound form of Rho (Ren et al., 1999). The results showed increased Rho activity in *Pyk2*-null cells (Fig. 6 A). The potential role of Rho activation was further tested by examining the effect of the Rho inhibitor C3-toxin on the stability of microtubules, and on podosome belt formation. The experiment presented in Fig. 6 B shows that C3-toxin treatment increased the stable pool of microtubules and induced the formation of a belt-like structure at the cell periphery of *Pyk2*-null osteoclasts. The stable pool of microtubules observed in *Pyk2*-null osteoclasts after treatment with C3 was also highly acetylated (Fig. 6 C). These results further indicate that enhanced Rho activity in *Pyk2*-null osteoclasts is responsible for the decrease in microtubule stability and acetylation, and impairment of podosome belt formation.

Lack of podosome belt in *Pyk2*-null osteoclasts cannot be rescued by activated Src

It was previously proposed that recruitment of Src by Pyk2 plays an important role in podosome belt formation and bone resorption in osteoclasts (Lakkakorpi et al., 2003; Miyazaki et al., 2004). Examination of the expression and activity of Src in wild-type and *Pyk2*-null osteoclasts revealed that, although the expression of Src was not altered in the absence of Pyk2 (Fig. 7 A), Src activity was reduced in both unstimulated and integrin-stimulated *Pyk2*-null osteoclasts (Fig. 7 B). However, podosome belt formation was not rescued in *Pyk2*-null osteoclasts that were microinjected with expression vector for activated Src (Src-Y527F) (Fig. 7 C), suggesting that the Pyk2-dependent pathway leading to microtubule-dependent podosome belt and sealing zone formation in osteoclasts is, by and large, a Src-independent process.

Published September 10, 2007

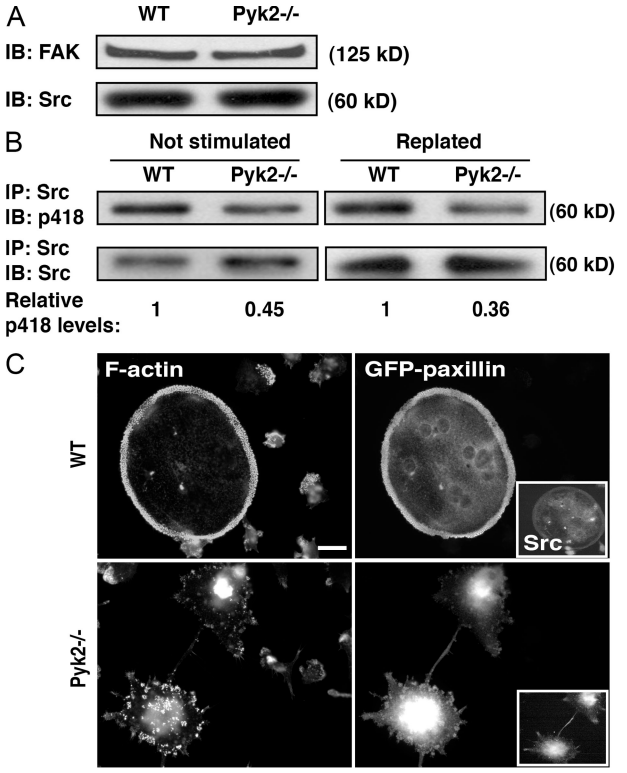

Figure 7. **Lack of podosome belt in *Pyk2*-null osteoclasts cannot be rescued by activated Src.** (A) Immunoblotting of lysates from wild-type or *Pyk2*-null osteoclasts with anti-FAK or anti-Src antibodies. (B) Left panels: Src was immunoprecipitated with anti-Src antibodies from lysates of wild-type or *Pyk2*-null osteoclasts followed by immunoblotting with either anti-pY418 antibodies directed against Src autophosphorylation site (top) or with anti-Src antibodies for detection of the total amount immunoprecipitated Src (bottom). Right: wild-type or *Pyk2*-null osteoclasts were suspended by EDTA treatment. After 30 min the suspended cells were attached to serum-coated plates for 1 h. Cell lysates were subjected to immunoprecipitation with anti-Src antibodies followed by immunoblotting with either anti-pY418 or anti-Src antibodies. The ratio between activated Src to total Src was determined by densitometry. (C) Wild-type and *Pyk2*-null osteoclasts were microinjected with expression vectors for Src-Y527F and GFP-paxillin as expression control. Cells were fixed, permeabilized, and labeled with anti-Src antibodies or with rhodamine-phalloidin. More than 75% of the cells expressing Y527F-Src and GFP-paxillin did not show any podosome belt or rings. The remaining cells showed small rings, but no belt was seen in any of the cells. Bar, 15 μm.

The Pyk2-ΔFAT mutant does not rescue podosome belt formation and bone resorption

To determine which Pyk2 domain(s) regulate podosome belt formation, we tested the ability of several Pyk2 mutants to rescue podosome belt formation in *Pyk2*-null osteoclasts. We tested Pyk2-Y402F, an autophosphorylation site mutant that does not bind Src; Pyk2-K457A, a kinase-negative mutant; Pyk2-ΔFAT (aa 1–868), a deletion mutant devoid of the FAT domain; Pyk2-ΔFERM (aa 381–1009), a deletion mutant that lacks the FERM domain; and, as a control, Pyk2-WT (Fig. 8 A). The different mutants were transiently expressed in HEK293 cells and their tyrosine kinase activity was analyzed by immunoblotting with antibodies specific for phosphorylated Tyr402 of Pyk2. All mutants except Pyk2-Y402F and Pyk2-K457A showed similar levels of autophosphorylation (Fig. S2 a, available at http://www.jcb.org/cgi/content/full/jcb.200701148/DC1). As expected,

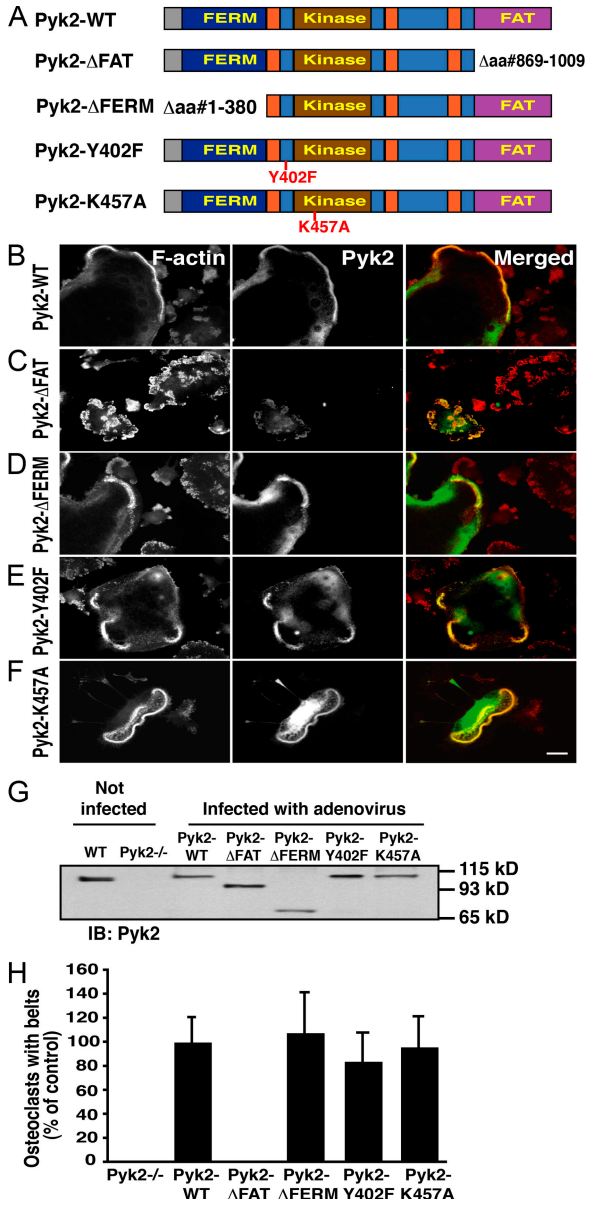

Figure 8. **The Pyk2-ΔFAT mutant does not rescue podosome belt formation.** (A) Schematic representation of Pyk2 mutants used in this study. Pyk2-WT, wild-type; Pyk2-ΔFAT, deletion mutant lacking the FAT domain (aa 869–1009); Pyk2-ΔFERM, deletion mutant lacking the FERM domain of (aa 1–380); Pyk2-Y402F, point mutation in Src SH2 domain binding site; Pyk2-K457A, a kinase negative mutant. (B–F) *Pyk2*-null osteoclasts were microinjected with expression vectors for wild-type (b) or different Pyk2 mutants (C–F). Cells were fixed, permeabilized, and labeled with anti-Pyk2 antibodies or rhodamine-phalloidin. Right panels show merged images (Pyk2 in green, F-actin in red). Bar, 15 μm. (G) *Pyk2*-null osteoclasts were infected with adenovirus carrying wild-type or Pyk2 mutants. Cells were lysed and the expression of Pyk2 proteins was revealed by immunoblotting with anti-Pyk2 antibodies and compared with the expression level of endogenous Pyk2 in wild-type osteoclasts. (H) *Pyk2*-null osteoclasts were infected with adenovirus carrying wild-type or Pyk2 mutants, and the number of cells bearing podosome belts at the cell periphery was counted. Results are presented as a percentage of control (WT-Pyk2). 800 cells were counted for each group.

Pyk2-WT, Pyk2-ΔFAT, and Pyk2-ΔFERM formed a complex with Src, whereas the Pyk2-Y402F and Pyk2-K457A mutants failed to bind Src to a substantial degree (Fig. S2, b and c).

Published September 10, 2007

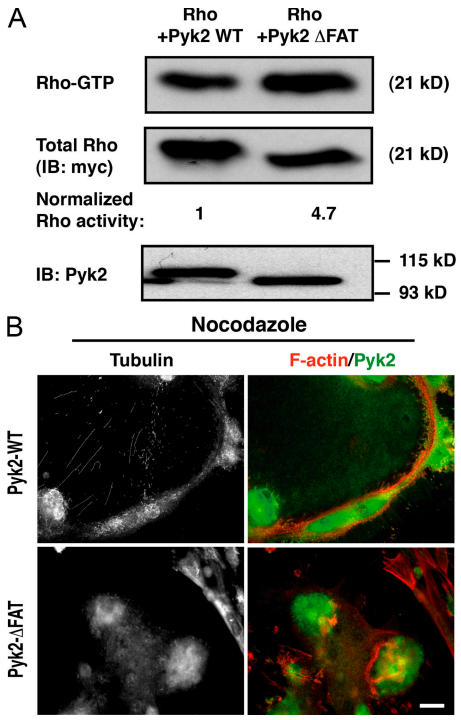

Figure 9. **Expression of Pyk2-ΔFAT mutant does not rescue Rho activation and microtubule acetylation in *Pyk2*-null osteoclasts.** (A) HEK293 cells were transfected with expression vectors for WT-Pyk2 together with myc-tagged Rho or with expression vectors for ΔFAT-Pyk2 together with myc-tagged Rho. Analysis of Rho activity was performed as described in Fig. 6. Shown is a representative of two experiments. (B) *Pyk2*-null osteoclasts infected with adenovirus carrying either wild-type or the ΔFAT-Pyk2 mutant were treated with 2 μM nocodazole for 45 min, after which the cells were fixed, permeabilized, and labeled with anti-tubulin, rhodamine-phalloidin (red), or anti-Pyk2 antibodies (green).

We next examined the ability of the different mutants to rescue podosome belt formation in *Pyk2*-null osteoclasts. Expression vectors for the different mutants were microinjected into osteoclasts from *Pyk2*$^{-/-}$ mice, and the cells were stained with fluorescently labeled phalloidin and anti-Pyk2 antibodies. Microinjection of Pyk2-WT cDNA completely rescued podosome belt formation in *Pyk2*-null osteoclasts (Fig. 8 B), providing further evidence that Pyk2 is required for the formation of the peripheral podosome belt in osteoclasts. Similar results were observed when *Pyk2*-null osteoclasts were microinjected with Pyk2-ΔFERM, Pyk2-Y402F, or Pyk2-K457A cDNAs (Fig. 8, D–F). In contrast, podosome belt formation was not observed in *Pyk2*-null osteoclasts that were microinjected with Pyk2-ΔFAT. Instead, podosome clusters and small rings were seen throughout the microinjected osteoclasts (Fig. 8 C). Examination of the cellular distribution of ectopically expressed Pyk2 molecules showed, however, that both wild-type and all mutant Pyk2 were confined to actin-containing podosomes, including the Pyk2-ΔFAT mutant (Fig. S3, available at http://www.jcb.org/cgi/content/full/jcb.200701148/DC1).

Similar results were obtained when *Pyk2*-null osteoclasts were infected with adenovirus containing wild-type Pyk2 or the different Pyk2 mutants, and matched for expression levels of endogenous Pyk2 (Fig. 8 G). Comparison of the infected cells demonstrated that only Pyk2-ΔFAT failed to induce belt formation in comparison to belt formation induced by wild-type Pyk2 (Fig. 8 H). In agreement with that, expression of Pyk2-ΔFAT was not able to either restore Rho activation or stabilization of microtubules, as demonstrated by a nocodazole-resistance assay (Fig. 9, A and B, respectively). The lack of a podosome belt in *Pyk2*-null osteoclasts infected with the Pyk2-ΔFAT virus correlated with the absence of sealing zone in these cells after replating on dentin, as shown in Fig. 10 A.

The effect of Pyk2 mutants on osteoclast function was then examined in a resorption assay. Expression of Pyk2-ΔFERM in *Pyk2*-null osteoclasts completely rescued their bone-resorbing activity. On the other hand, the bone-resorbing activity was only partially restored by the Pyk2-Y402F and Pyk2-K457A mutants, notwithstanding the complete restoration of podosome belt formation by these mutants (Fig. 10). The area, depth, and volume of pits formed by *Pyk2*-null osteoclasts that were infected with Pyk2-ΔFAT virus were significantly reduced (Fig. 10, B–D), further confirming the importance of the FAT domain in promoting osteoclast function. These results suggest that although Src recruitment and Pyk2 kinase activity contribute to bone resorption, the FAT domain of Pyk2 plays a major role in podosome organization and bone resorption.

Discussion

We have previously reported that Pyk2 deficiency results in impairment of macrophage function (Okigaki et al., 2003). Here, we report that Pyk2 deficiency also leads to osteopetrotic phenotype by impairment in the bone-resorbing activity of osteoclasts. In addition, experiments are presented demonstrating that Rho activity, microtubule stabilization and podosome organization are altered in *Pyk2*-null osteoclasts. Although we cannot exclude the contribution of osteoblasts to the increased bone mass, the accumulation of cartilage remnants despite elevated osteoclast numbers confirm in vivo an impairment in osteoclast function. Furthermore, the in vitro experiments establish the fact that *Pyk2*-null osteoclasts are deficient in cytoskeletal organization and bone resorption, in a cell-autonomous manner. Thus, Pyk2 plays a critical role in podosome organization and osteoclast function.

Analysis of the cellular distribution of Pyk2 by immunofluorescence microscopy showed that Pyk2 is preferentially localized in the periphery of osteoclasts in a region that overlaps with the podosome belt, when the cells are plated on glass, or the similar sealing zone, when plated on mineralized bone. Comparison of the cellular distribution of actin revealed that Pyk2 deficiency results in impairment in the formation of podosome belt and sealing zone in osteoclasts. Instead, *Pyk2*-null osteoclasts contain multiple podosome clusters and small podosome rings throughout the cell.

Given that a link has been established between microtubules and actin organization (Waterman-Storer and Salmon, 1999), we have explored the possibility of whether microtubule distribution and/or dynamics were altered in osteoclasts deficient in Pyk2. Immunofluorescence studies showed that the cellular distribution of microtubules is significantly altered in *Pyk2*-null osteoclasts; while *Pyk2*-null osteoclasts retained the radial network, they lost their circular microtubule network that is usually

Published September 10, 2007

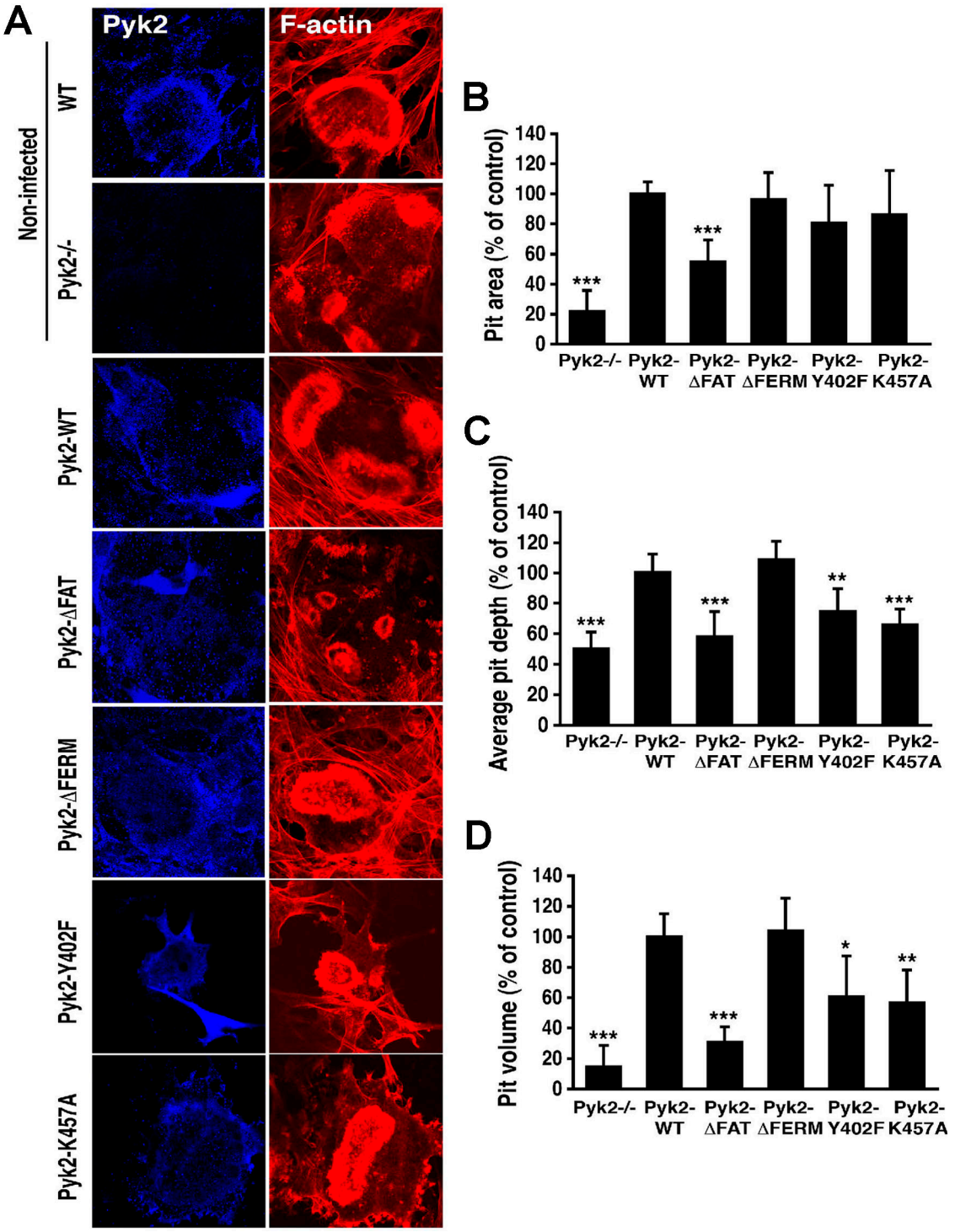

Figure 10. **Reduced bone resorption in *Pyk2*-null osteoclasts expressing a Pyk2-ΔFAT mutant.** (A) *Pyk2*-null osteoclasts were infected with adenovirus carrying either wild-type or Pyk2 mutants. The infected cells were detached and replated on dentin for 36 h, fixed, permeabilized, and labeled with rhodamine-phalloidin (red) or with anti-Pyk2 antibodies (blue). Noninfected wild-type and *Pyk2*-null osteoclasts are shown in the top two panels as control. (B) Infected *Pyk2*-null osteoclasts were detached and replated on dentin for 48 h and allowed to excavate pits. Pit volume was measured and analyzed using violet laser color 3D profile confocal microscope. Results were normalized to the number of TRAP-positive cells in each sample, and are represented as means ± SD, relative to cells infected with Pyk2-WT adenovirus. $n = 6$ from two independent experiments. *, $P < 0.05$; **, $P < 0.01$, ***, $P < 0.001$, as determined by *t* test.

seen at the periphery of osteoclasts. The stable, nocodazole-resistant pool of microtubules that has previously been implicated in mediating the transition from podosome clusters and rings into the peripheral podosome belt (Destaing et al., 2003), was nearly eliminated in *Pyk2*-null osteoclasts. Consistent with this finding, the acetylation of microtubules, which correlates with microtubule stabilization, was also markedly reduced in *Pyk2*-null osteoclasts. Microtubule acetylation is controlled in

Published September 10, 2007

part by the activity of histone and microtubule deacetylase HDAC6, which in turn is regulated by the small GTPase Rho (Destaing et al., 2005). We found that Pyk2 deficiency results in increased Rho activity, and established that this leads to reduced microtubule acetylation and reduced microtubule stability. We propose that Pyk2 may function as an upstream inhibitor of this signaling pathway in osteoclasts, which ultimately allows the transition of podosomes from the center of the cells, where they form clusters and small internal podosome rings, to the periphery, where they form a podosome belt and sealing zone, a structure necessary for efficient bone resorption.

During directional migration of fibroblasts, the stable pool of microtubules becomes oriented toward the leading edge of the cell (Gundersen and Bulinski, 1988). Moreover, the microtubules of fibroblasts are post-translationally modified, and as in osteoclasts, the modifications are associated with enhanced microtubule stability (Westermann and Weber, 2003). In addition, FAK activation in the leading edge of fibroblasts leads to enhanced Rho activity and microtubule stability (Palazzo et al., 2004). In osteoclasts, on the other hand, enhanced stimulation of microtubule stability and podosome organization are controlled by Pyk2-mediated reduced Rho activation. Although the reason for this difference is unknown, this could be explained by different effects of Pyk2 and FAK on Rho activation, or, as suggested before (Destaing et al., 2005), could be due to cell type–specific effects of Rho inhibition on microtubule stability.

Ectopic expression of wild-type Pyk2 in *Pyk2*-null osteoclasts, at levels comparable to endogenous expression of the protein in wild-type cells, rescued the formation of a podosome belt and sealing zone as well as bone resorption. The cellular responses were also rescued by expression of a deletion mutant of Pyk2 lacking the FERM domain. Podosome belt formation was rescued by expression of a kinase-negative Pyk2 mutant (K457A) and by a point mutant in a tyrosine phosphorylation site (Y402F) that is responsible for mediating complex formation with Src. In contrast, a deletion mutant devoid of the FAT domain was not able to rescue normal responses in *Pyk2*-null osteoclasts, emphasizing the importance of this domain in the regulation of microtubule stability and podosome organization in these cells.

It was previously shown that the FAT domain is responsible for Pyk2 localization in focal contacts of fibroblasts and HeLa cells (Schaller and Sasaki, 1997; Xiong et al., 1998; Litvak et al., 2000). However, a deletion mutant of Pyk2 devoid of the FAT domain remains localized around the actin-rich podosome core in *Pyk2*-null osteoclasts, suggesting that the inability of mutant protein to rescue podosome belt or sealing zone formation and bone resorption are not caused by a defect in cellular distribution. The FAT domain of Pyk2 may participate in podosome belt formation by regulating the activities of guanine nucleotide exchange factors or GTPase-activating proteins (GAPs) that regulate Rho activity, resulting in the control of acetylation and stabilization of microtubules in the pathways mentioned earlier in the Discussion, thereby regulating osteoclast cytoskeletal organization and bone resorption.

The rescue of Pyk2-dependent podosome belt formation in *Pyk2*-null osteoclasts by the kinase-negative Pyk2 mutant suggests that Pyk2 may function as a platform for recruitment and assembly of signaling proteins in addition to its function as tyrosine kinase. Accordingly, other tyrosine kinases may compensate for the loss of intrinsic tyrosine kinase activity of Pyk2 by trans-phosphorylation of key tyrosine residues that function as docking sites for signaling proteins. Pyk2 may also recruit signaling proteins in a phosphorylation-independent manner through interactions mediated by its proline-rich region with SH3 domain–containing signaling proteins.

The effect of overexpression of Pyk2-Y402F in wild-type osteoclasts was previously described (Lakkakorpi et al., 2003; Miyazaki et al., 2004), demonstrating that osteoclasts that overexpress this mutant fail to form podosome belt and show reduced bone resorption in vitro. Consistently, as demonstrated in our paper, in the absence of endogenous Pyk2, Pyk2-Y402F can partially restore bone resorption, but completely restores the formation of a peripheral podosome belt. This, together with the finding that microinjection of Src-Y527F into *Pyk2*-null osteoclasts cannot rescue podosome belt formation, suggests that Pyk2 may mediate two separate pathways: a Rho-dependent pathway that regulates microtubule-dependent podosome organization, and a Src-dependent pathway that may be involved in other functions related to bone resorption, such as actin dynamics, cell attachment, or ruffled border formation.

We also show that actin dynamics are altered in the absence of Pyk2; the rate of incorporation of GFP-actin into podosomes in photobleached areas is slowed down by an approximately twofold in the absence of Pyk2. Previous reports have interpreted slower actin fluxes as an indication of reduced actin polymerization (Destaing et al., 2003), which could result from the inhibition of actin polymerizing proteins or from enhanced actin severing along the filaments. The role of actin polymerization in podosome formation and function is still poorly understood, but it has been suggested that polymerization induces a force that pushes the cell membrane toward the substrate (Prass et al., 2006; Footer et al., 2007), a process that may also be essential for attachment of osteoclasts to their substrate and therefore to bone resorption.

Finally, the ruffled border is a membrane-rich organelle that is surrounded by the sealing zone, and through which protons and proteolytic enzymes are secreted to resorb the bone matrix. We have observed in *Pyk2*-null osteoclasts a shorter and irregular ruffled border structure and defective translocation of the proton pump to this region in *Pyk2*-null osteoclasts (unpublished data). This may explain the shallow pits formed by *Pyk2*-null osteoclasts, and may suggest additional, yet unknown roles of Pyk2 in osteoclast function and bone resorption.

In conclusion, this study demonstrates that Pyk2 is required for normal organization of the cytoskeleton in osteoclasts, and bone resorption. In the absence of Pyk2, Rho activity is increased, microtubule acetylation and stabilization are decreased, and transition of podosomes to the periphery of the cell is prevented.

Materials and methods

Generation of knockout mice

Generation of *Pyk2*$^{-/-}$ mice was described previously (Okigaki et al., 2003). Animals were handled in accordance with the guidelines of Yale University Institutional Animal Care and Use Committee.

Published September 10, 2007

Histomorphometry

Bone samples were collected for histomorphometric analysis at 2 and 10 wk of age. Double-fluorochrome labeling was performed in 10-wk-old mice as described previously (Sims et al., 2000); animals were injected with calcein (20 mg/kg body weight) followed by the same dose of demeclocycline at 10 and 3 d before tissue collection, respectively. Tibiae and femora were collected, fixed in 3.7% formaldehyde in PBS, and embedded in methylmethacrylate as described previously (Sims et al., 2000). 5-μm sections were stained with Toluidine blue or Alcian blue or by the Von Kossa method, or analyzed unstained for fluorochrome labels. Histomorphometric analysis was performed according to standard procedures using the Osteomeasure system (OsteoMetrics, Inc.) in the proximal tibiae. Tibial cortical thickness and periosteal mineral appositional rates were measured as described previously (Sims et al., 2000). Femoral length and width were determined from contact X-rays that were scanned and measured using NIH Image 2.0.

Reagents

Mouse MCSF and RANKL were obtained from R&D systems. Nocodazole was obtained from Sigma-Aldrich. Cell-permeable C3 was obtained from Cytoskeleton, Inc. Monoclonal anti-Pyk2 and anti-FAK antibodies were purchased from Transduction Laboratories. Anti-pY402 Pyk2 and anti-pY418 Src antibodies were from Biosource International. Anti-v-Src monoclonal antibody was from Calbiochem. Monoclonal anti-RhoA antibody (26C4) was purchased from Santa Cruz Biotechnology, Inc. Anti–α-tubulin was from Abcam. Anti-acetylated tubulin was from Sigma-Aldrich. Anti-actin antibody was from Chemicon. Texas red– and rhodamine-conjugated phalloidin and secondary antibodies for immunofluorescence were purchased from Invitrogen.

Plasmids and recombinant adenovirus

pEGFP-actin was obtained from CLONTECH Laboratories, Inc. pShuttle plasmids containing Pyk2-WT (wild-type Pyk2), Pyk2-Y402F (mutation in Src SH2-domain binding site), Pyk2-K457A (a kinase-negative mutant), Pyk2-ΔFAT (deletion mutant devoid of the FAT domain), and Pyk2-ΔFERM (deletion mutant devoid of the FERM domain) were used for transfection and microinjection experiments. Recombinant adenoviruses expressing the above mutants were prepared by recombination of the above plasmids using the Adenovator Vector System (Qbiogene) according to the manufacturer's instructions.

Preparation of osteoclast cultures

Authentic osteoclasts from 2–4-d-old neonatal mice and co-culture osteoclasts from 6–8-wk-old mice were prepared as described previously (Sanjay et al., 2001). Spleen leukocyte cells were prepared and differentiated in culture using MCSF and RANK ligand as described previously (Destaing et al., 2003).

Microinjection

Mouse spleen cell–derived osteoclasts were transferred to observation medium (α-MEM without bicarbonate containing 10% fetal calf serum, 20 mM Hepes, 20 ng/ml M-CSF, and 20 ng/ml of soluble recombinant RANK-L). Intranuclear microinjection of cDNAs (0.2 mg/ml in water) was performed at room temperature on an inverted microscope (model IX 71; Olympus) using an InjectMan NI2 micromanipulator and a FemtoJet Microinjector (Eppendorf). After microinjection, cells were maintained at 37°C and 5% CO_2 for at least 6 h in differentiation medium before imaging.

Time-lapse microscopy

Osteoclasts were differentiated in 35-mm glass-bottom Petri dishes, then transferred to observation medium. After microinjection of DNA coding for GFP-tagged actin, the dishes were placed on a 37°C heated stage (Carl Zeiss MicroImaging, Inc.) and cells were imaged with a microscope (Axiovert 200M; Carl Zeiss MicroImaging, Inc.) containing a 40× (NA 1.0) Plan-Apochromat objective, a 63× (NA 1.4) Plan NeoFluor objective, and equipped with a MicroMax 5-MHz camera (Princeton Instruments, Inc.). Meta Imaging Series 7.0 (Universal Imaging Corp.) was used to mount AVI movies from image stacks. Extracted images from stacks were processed (brightness/contrast adjustment) with Adobe Photoshop 6.0 and ImageJ.

Confocal microscopy and FRAP measurements

For immunofluorescence, cells were fixed with 4% paraformaldehyde diluted into PBS, pH 7.4, processed as described previously (Ory et al., 2000), and imaged with a microscope (LSM Meta; Carl Zeiss MicroImaging, Inc.) using a 63× (NA 1.4) Plan NeoFluor objective. To prevent cross-contamination between fluorochromes, each channel was imaged sequentially using the multi-track recording module before merging.

FRAP experiments were performed on osteoclasts prepared as for regular videomicroscopy experiments using the same confocal setup described previously. Bleaching time (3.2 s), acquisition rate (1 image every 547 ms), and bleaching area were the same for all experiments. Image extraction was performed with Meta Imaging Series (Universal Imaging Corp.). The fluorescence recovery was measured only within podosome cores that existed during the whole recovery time. Fluorescence intensity at each time point was normalized to the starting fluorescence intensity (prebleach). To analyze recovery kinetics, FRAP measurements were fitted to a single exponential curve (performed with Igor Pro 4.0; WaveMetrics) as described in Meyvis et al. (1999).

Immunoprecipitation and immunoblotting experiments

HEK293 cells were transfected using Lipofectamine (Invitrogen) according to the manufacturer's instructions. Immunoprecipitation and immunoblotting were preformed as described previously (Okigaki et al., 2003).

GTP-Rho pull-down assay

GST fusion protein containing the Rho binding domain of rhotekin (RBD) was produced and used for pull-down experiments with osteoclast lysates as described previously (Ren et al., 1999).

Pit formation assay

Pit resorption assay was preformed as described previously (Miyazaki et al., 2004). Three-dimensional profiles of resorbed pits were characterized by using a reflective confocal laser scanning microscope (RCLSM) (model VK8510; Keyence) under the 50× objective lens (NA 0.8) interfaced via a CCD camera to "Virtual view 3D (version 2.5)" for making the three-dimensional reconstruction image profile. The images were displayed at a resolution of 1024 × 768 pixels. Quantitative analysis of resorbed pit number, area, and volume were performed using Win ROOF image-analyzing software (version 5.5; Mitani Corp.) (Aoki et al., 2006).

Online supplemental material

Fig. S1 shows the distribution of paxillin in wild-type and *Pyk2*-null osteoclasts. Fig. S2 shows expression of the different mutants of Pyk2, their autophosphorylation status, and their binding to Src. Fig. S3 shows the cellular distribution of actin and Pyk2 in osteoclasts microinjected with the different Pyk2 mutants. Fig. S4 shows localization of microinjected mDia2-GFP in wild-type and *Pyk2*-null osteoclasts. Online supplemental material is available at http://www.jcb.org/cgi/content/full/jcb.200701148/DC1.

We are grateful to Dr. William C. Horne for critically reading the manuscript, Francisco Tomé for maintaining the mouse colony, Dr. Hiroaki Saito and Dr. Naoyuki Takahashi for providing dentin slices, and Dr. Riku Kiviranta for technical help.

This work was supported by National Institutes of Health grants AR 051448, AR 051886, and P50 AR054086 (to J. Schlessinger), and AR 042927 and DE 004724 (to R. Baron); grant no. 19390471 from the Ministry of Education, Science and Culture in Japan (to Dr. Keiichi Ohya and Dr. Kazuhiro Aoki); and by the Center of Excellence Program for Frontier Research on Molecular Destruction and Reconstruction of Tooth and Bone (to N. Alles). Hava Gil-Henn was supported by EMBO long-term postdoctoral fellowship.

Submitted: 26 January 2007
Accepted: 9 August 2007

References

Aoki, K., H. Saito, C. Itzstein, M. Ishiguro, T. Shibata, R. Blanque, A.H. Mian, M. Takahashi, Y. Suzuki, M. Yoshimatsu, et al. 2006. A TNF receptor loop peptide mimic blocks RANK ligand-induced signaling, bone resorption, and bone loss. *J. Clin. Invest.* 116:1525–1534.

Axelrod, D., D.E. Koppel, J. Schlessinger, E. Elson, and W.W. Webb. 1976. Mobility measurement by analysis of fluorescence photobleaching recovery kinetics. *Biophys. J.* 16:1055–1069.

Destaing, O., F. Saltel, J.C. Geminard, P. Jurdic, and F. Bard. 2003. Podosomes display actin turnover and dynamic self-organization in osteoclasts expressing actin-green fluorescent protein. *Mol. Biol. Cell.* 14:407–416.

Destaing, O., F. Saltel, B. Gilquin, A. Chabadel, S. Khochbin, S. Ory, and P. Jurdic. 2005. A novel Rho-mDia2-HDAC6 pathway controls podosome patterning through microtubule acetylation in osteoclasts. *J. Cell Sci.* 118:2901–2911.

Published September 10, 2007

Dikic, I., I. Dikic, and J. Schlessinger. 1998. Identification of a new Pyk2 isoform implicated in chemokine and antigen receptor signaling. *J. Biol. Chem*. 273:14301–14308.

Duong, L.T., P.T. Lakkakorpi, I. Nakamura, M. Machwate, R.M. Nagy, and G.A. Rodan. 1998. PYK2 in osteoclasts is an adhesion kinase, localized in the sealing zone, activated by ligation of alpha(v)beta3 integrin, and phosphorylated by src kinase. *J. Clin. Invest.* 102:881–892.

Duong, L.T., I. Nakamura, P.T. Lakkakorpi, L. Lipfert, A.J. Bett, and G.A. Rodan. 2001. Inhibition of osteoclast function by adenovirus expressing antisense protein-tyrosine kinase 2. *J. Biol. Chem.* 276:7484–7492.

Footer, M.J., J.W. Kerssemakers, J.A. Theriot, and M. Dogterom. 2007. Direct measurement of force generation by actin filament polymerization using an optical trap. *Proc. Natl. Acad. Sci. USA.* 104:2181–2186.

Gundersen, G.G., and J.C. Bulinski. 1988. Selective stabilization of microtubules oriented toward the direction of cell migration. *Proc. Natl. Acad. Sci. USA*. 85:5946–5950.

Helfrich, M.H., D.C. Aronson, V. Everts, R.H. Mieremet, E.J. Gerritsen, P.G. Eckhardt, C.G. Groot, and J.P. Scherft. 1991. Morphologic features of bone in human osteopetrosis. *Bone.* 12:411–419.

Hollberg, K., K. Hultenby, A. Hayman, T. Cox, and G. Andersson. 2002. Osteoclasts from mice deficient in tartrate-resistant acid phosphatase have altered ruffled borders and disturbed intracellular vesicular transport. *Exp. Cell Res.* 279:227–238.

Lakkakorpi, P.T., A.J. Bett, L. Lipfert, G.A. Rodan, and T. Duong le. 2003. PYK2 autophosphorylation, but not kinase activity, is necessary for adhesion-induced association with c-Src, osteoclast spreading, and bone resorption. *J. Biol. Chem*. 278:11502–11512.

Lev, S., H. Moreno, R. Martinez, P. Canoll, E. Peles, J.M. Musacchio, G.D. Plowman, B. Rudy, and J. Schlessinger. 1995. Protein tyrosine kinase PYK2 involved in Ca(2+)-induced regulation of ion channel and MAP kinase functions. *Nature.* 376:737–745.

Linder, S., and M. Aepfelbacher. 2003. Podosomes: adhesion hot-spots of invasive cells. *Trends Cell Biol.* 13:376–385.

Litvak, V., D. Tian, Y.D. Shaul, and S. Lev. 2000. Targeting of PYK2 to focal adhesions as a cellular mechanism for convergence between integrins and G protein-coupled receptor signaling cascades. *J. Biol. Chem.* 275:32736–32746.

Luxenburg, C., D. Geblinger, E. Klein, K. Anderson, D. Hanein, B. Geiger, and L. Addadi. 2007. The architecture of the adhesive apparatus of cultured osteoclasts: from podosome formation to sealing zone assembly. *PLoS ONE.* 2:e179.

McHugh, K.P., K. Hodivala-Dilke, M.H. Zheng, N. Namba, J. Lam, D. Novack, X. Feng, F.P. Ross, R.O. Hynes, and S.L. Teitelbaum. 2000. Mice lacking beta3 integrins are osteosclerotic because of dysfunctional osteoclasts. *J. Clin. Invest.* 105:433–440.

Meyvis, T.K., S.C. De Smedt, P. Van Oostveldt, and J. Demeester. 1999. Fluorescence recovery after photobleaching: a versatile tool for mobility and interaction measurements in pharmaceutical research. *Pharm Res*. 16:1153–1162.

Miyazaki, T., A. Sanjay, L. Neff, S. Tanaka, W.C. Horne, and R. Baron. 2004. Src kinase activity is essential for osteoclast function. *J. Biol. Chem.* 279:17660–17666.

Okigaki, M., C. Davis, M. Falasca, S. Harroch, D.P. Felsenfeld, M.P. Sheetz, and J. Schlessinger. 2003. Pyk2 regulates multiple signaling events crucial for macrophage morphology and migration. *Proc. Natl. Acad. Sci. USA*. 100:10740–10745.

Ory, S., Y. Munari-Silem, P. Fort, and P. Jurdic. 2000. Rho and Rac exert antagonistic functions on spreading of macrophage-derived multinucleated cells and are not required for actin fiber formation. *J. Cell Sci.* 113:1177–1188.

Palazzo, A.F., C.H. Eng, D.D. Schlaepfer, E.E. Marcantonio, and G.G. Gundersen. 2004. Localized stabilization of microtubules by integrin- and FAK-facilitated Rho signaling. *Science.* 303:836–839.

Pfaff, M., and P. Jurdic. 2001. Podosomes in osteoclast-like cells: structural analysis and cooperative roles of paxillin, proline-rich tyrosine kinase 2 (Pyk2) and integrin alphaVbeta3. *J. Cell Sci.* 114:2775–2786.

Prass, M., K. Jacobson, A. Mogilner, and M. Radmacher. 2006. Direct measurement of the lamellipodial protrusive force in a migrating cell. *J. Cell Biol.* 174:767–772.

Ren, X.D., W.B. Kiosses, and M.A. Schwartz. 1999. Regulation of the small GTP-binding protein Rho by cell adhesion and the cytoskeleton. *EMBO J.* 18:578–585.

Richardson, A., and T. Parsons. 1996. A mechanism for regulation of the adhesion-associated proteintyrosine kinase pp125FAK. *Nature.* 380:538–540.

Sanjay, A., A. Houghton, L. Neff, E. DiDomenico, C. Bardelay, E. Antoine, J. Levy, J. Gailit, D. Bowtell, W.C. Horne, and R. Baron. 2001. Cbl associates with Pyk2 and Src to regulate Src kinase activity, alpha(v)beta(3) integrin-mediated signaling, cell adhesion, and osteoclast motility. *J. Cell Biol.* 152:181–195.

Schaller, M.D., and T. Sasaki. 1997. Differential signaling by the focal adhesion kinase and cell adhesion kinase beta. *J. Biol. Chem.* 272:25319–25325.

Schlaepfer, D.D., C.R. Hauck, and D.J. Sieg. 1999. Signaling through focal adhesion kinase. *Prog. Biophys. Mol. Biol.* 71:435–478.

Sims, N.A., P. Clement-Lacroix, F. Da Ponte, Y. Bouali, N. Binart, R. Moriggl, V. Goffin, K. Coschigano, M. Gaillard-Kelly, J. Kopchick, et al. 2000. Bone homeostasis in growth hormone receptor-null mice is restored by IGF-I but independent of Stat5. *J. Clin. Invest.* 106:1095–1103.

Soriano, P., C. Montgomery, R. Geske, and A. Bradley. 1991. Targeted disruption of the c-src proto-oncogene leads to osteopetrosis in mice. *Cell.* 64:693–702.

Takahashi, N., H. Yamana, S. Yoshiki, G.D. Roodman, G.R. Mundy, S.J. Jones, A. Boyde, and T. Suda. 1988. Osteoclast-like cell formation and its regulation by osteotropic hormones in mouse bone marrow cultures. *Endocrinology.* 122:1373–1382.

Turksen, K., J. Kanehisa, M. Opas, J.N. Heersche, and J.E. Aubin. 1988. Adhesion patterns and cytoskeleton of rabbit osteoclasts on bone slices and glass. *J. Bone Miner. Res.* 3:389–400.

Walker, D.G. 1975. Spleen cells transmit osteopetrosis in mice. *Science.* 190:785–787.

Waterman-Storer, C., and E. Salmon. 1999. Positive feedback interactions between microtubule and actin dynamics during cell motility. *Curr. Opin. Cell Biol.* 11:61–67.

Westermann, S., and K. Weber. 2003. Post-translational modifications regulate microtubule function. *Nat. Rev. Mol. Cell Biol.* 4:938–947.

Williams, L.M., and A.J. Ridley. 2000. Lipopolysaccharide induces actin reorganization and tyrosine phosphorylation of Pyk2 and paxillin in monocytes and macrophages. *J. Immunol.* 164:2028–2036.

Xiong, W.C., M. Macklem, and J.T. Parsons. 1998. Expression and characterization of splice variants of PYK2, a focal adhesion kinase-related protein. *J. Cell Sci.* 111:1981–1991.